

Higgs Physics at a Future e^+e^- Linear Collider

Markus Schumacher

Deutsches Elektronensynchrotron, DESY, Notkestr.85, 22603 Hamburg, Germany



This letter reviews the potential of a high luminosity e^+e^- linear collider (LC) in the precision study of the Higgs boson profile. The complementarity with the Large Hadron Collider (LHC) Higgs physics program is briefly discussed.

1 Introduction: The Quest for the Higgs

Unraveling the mechanism responsible for electroweak symmetry breaking and the generation of particle masses is one of the great scientific quests of high energy physics today. The Standard Model (SM) and its Supersymmetric (SUSY) extensions address this question by the Higgs mechanism¹. The first manifestation of the Higgs mechanism is represented by the existence of at least one Higgs boson. This motivates the large experimental effort for the Higgs boson search in the past and future decades. The findings of the finished LEP2 program are a preliminary lower limit on the SM Higgs boson mass of 114.1 GeV and the observation of a slight excess around 115 GeV, compatible with the background-only-hypothesis at a level of 3.4%². The hunt will continue at the Tevatron $p\bar{p}$ -collider at $\sqrt{s} \approx 2$ TeV, covering the mass range with 3σ evidence up to 180 GeV with 30 fb^{-1} per experiment³. In pp -collisions at $\sqrt{s} = 14$ TeV at the LHC the entire SM mass range will be covered with at least 5σ evidence with 30 fb^{-1} per experiment⁴. For the MSSM Higgs sector, at least one Higgs boson can be observed for the entire parameter space with an integrated luminosity of 300 fb^{-1} ⁴. However, the discovery at these hadron machines relies on the identification of specific Higgs decay modes. At the LC the Higgs boson can be observed in the Higgs-strahlung process $e^+e^- \rightarrow ZH$ with $Z \rightarrow \ell^+\ell^-$, independently of its decay mode by a distinctive peak in the di-lepton recoil mass distribution. A data set of 500 fb^{-1} at $\sqrt{s} = 350$ GeV, corresponding to 2 to 3 years of running, provides a sample of 4600-2300 Higgs particles for M_H between 120 and 200 GeV in this channel⁵.

After the discovery the full validation of the Higgs mechanism requires an accurate determination of the Higgs bosons production and decay properties. The potential of the LC in the precision study of the Higgs boson profile is reviewed in Section 2^a. The prospects for the investigation of the MSSM Higgs sector are discussed in Section 3 and finally the complementarity with the LHC is outlined in Section 4.

^aThe results discussed here are mainly based on the ECFA/DESY study as summarised in⁵. In the meantime similar studies have been performed and documented in other regional Higgs working groups for SNOWMASS 2001⁶.

2 Higgs Boson Profile

2.1 Higgs Mass

The Higgs Mass M_H is the only unknown parameter left in the SM. Once its mass is known, the profile of the Higgs sector in the SM is uniquely determined. High precision is needed in order to discriminate between the SM and theories with an extended Higgs sector *e.g.* SUSY models. At the LC the Higgs mass can be best measured exploiting the kinematics in the Higgs-strahlung process $e^+e^- \rightarrow Z \rightarrow ZH$. The use of the recoil mass spectrum for leptonic Z decays ($Z \rightarrow e^+e^-, \mu^+\mu^-$) yields an accuracy of 110 MeV for 500 fb^{-1} , without any requirement on the Higgs boson decay⁷. The accuracy can be improved by identifying and reconstructing the Higgs decay mode and applying kinematic fits with constraints. For $M_H \leq 130 \text{ GeV}$ the dominant decay mode is into $b\bar{b}$, whereas for higher masses the WW^* channel becomes more important. Examples of reconstructed mass spectra are shown in Fig. 1. The combination of these measurements yields an accuracy between 40 and 80 MeV for M_H between 120 and 180 GeV for $\mathcal{L} = 500 \text{ fb}^{-1}$ ⁷.

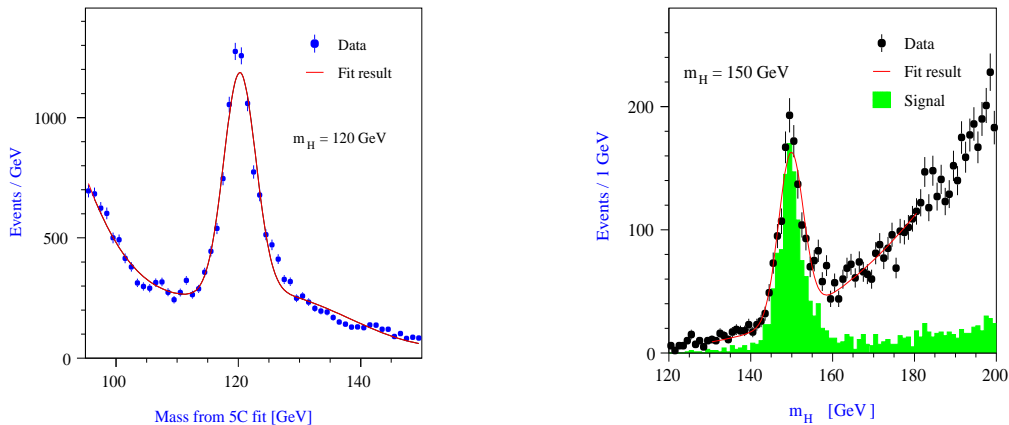


Figure 1: The Higgs boson mass reconstructed in the $H \rightarrow b\bar{b}, Z \rightarrow q\bar{q}$ channel for $M_H = 120 \text{ GeV}$ (left) and in the $H \rightarrow WW^*, Z \rightarrow q\bar{q}$ channel for $M_H = 150 \text{ GeV}$ (right).

2.2 Quantum Numbers

The spin, parity and charge-conjugation quantum numbers of the Higgs bosons can be determined at a LC in a model-independent way. The observation of Higgs boson production at the photon collider $\gamma\gamma \rightarrow H$ or of the decay $H \rightarrow \gamma\gamma$ would rule out $J = 1$ and require C to be positive. An scan of the threshold rise of the Higgs-strahlung cross-section and the measurement of the angular dependence of the Higgs production allow to determine J and P uniquely and to distinguish between a CP -even SM like Higgs boson (0^{++}), a CP -odd (0^{+-}) state A, and a CP -violating mixture denoted by Φ of the two⁸. A threshold scan with a luminosity of 20 fb^{-1} at three center-of-mass energies is sufficient to distinguish between the different rise expected for different spin assumptions⁹ (see Fig. 2 (left)). In a general model with two Higgs doublets (2HDM) the three neutral Higgs bosons correspond to arbitrary mixtures of CP eigenstates and their production and decay may exhibit CP violation. In this case, the amplitude for the Higgs-strahlung process can be described by adding a ZZA coupling with strength η to the SM matrix element. The squared amplitude is then given by $|\mathcal{M}_{Z\Phi}|^2 = |\mathcal{M}_{ZH}|^2 + 2\eta \text{Re}(\mathcal{M}_{ZH}^* \mathcal{M}_{ZA}) + \eta^2 |\mathcal{M}_{ZA}|^2$ ¹⁰. The first term corresponds to the SM cross-section, the second, linear in η , to the interference term, gives rise to CP -violating effects and the third term, quadratic in η and CP conserving, increases the total cross-section. The latter two change also the angular distributions of

the decay $Z \rightarrow f\bar{f}$. The information carried by these distributions has been analysed using the formalism of optimal observables for the $ZH \rightarrow \mu^+\mu^-X$ final state for $M_H = 120$ GeV, $\sqrt{s} = 350$ GeV and $\mathcal{L} = 500$ fb $^{-1}$. The accuracy on η has been found to be ≈ 0.03 ¹¹.

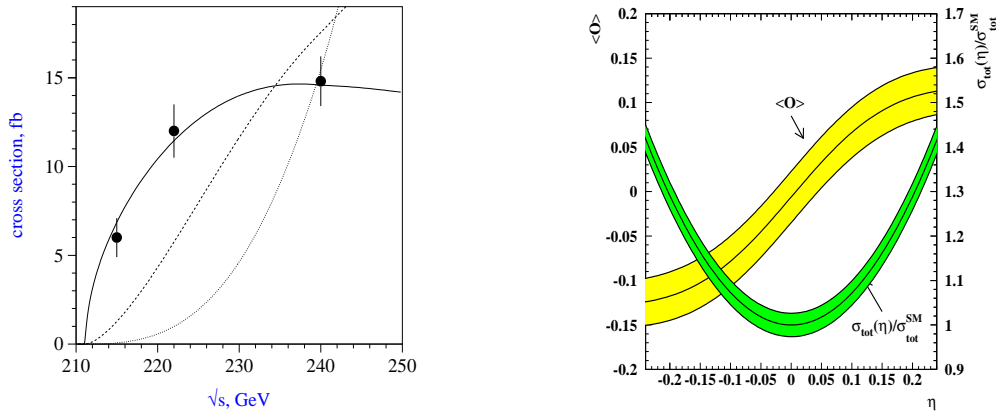


Figure 2: Left: Simulated measurement of the $e^+e^- \rightarrow ZH$ cross-section for $M_H = 120$ GeV with 20 fb $^{-1}$ at three center-of-mass energies compared to predictions for a spin-0 (full line), and examples of spin-1 (dashed line) and spin-2 (dotted line) particles. Right: The dependence of the expectation value of the optimal observable (light grey) and the total cross-section (dark grey) on η for $M_H = 120$ GeV, $\sqrt{s} = 350$ GeV and $\mathcal{L} = 500$ fb $^{-1}$. The shaded bands show the the 1σ uncertainties expected.

2.3 Couplings to Electroweak Gauge Bosons

The couplings to massive gauge bosons W and Z can be probed independently and best in the measurement of the production cross-sections for Higgs-strahlung ($e^+e^- \rightarrow Z \rightarrow ZH$), which is proportional to g_{HZZ}^2 , and WW -fusion ($e^+e^- \rightarrow H^0\nu_e\bar{\nu}_e$), which is proportional to g_{HWW}^2 .

The cross-section for the Higgs-strahlung process can be measured by analysing the mass spectrum of the system recoiling against leptonic decays of the Z (see Fig. 3 (left)). This provides a cross-section determination independent of the Higgs boson decay modes. The accuracy achieved in detailed studies is between 2.5% and 3.0% for Higgs masses between 120 and 160 GeV⁷.

The cross-section for WW -fusion can be determined in the $b\bar{b}\nu\bar{\nu}$ final state, where these events can be well separated from the Higgs-strahlung final state and the background processes by exploiting the different spectra of the $\nu\bar{\nu}$ invariant mass (see Fig. 3 (right)). From a simultaneous fit of the above contributions the cross-section can be extracted with an accuracy between 3% and 13% for M_H between 120 and 160 GeV¹².

The measurement of the branching ratio $H \rightarrow WW^*$ provides an alternative means to access the g_{HWW} coupling. The experimental study has been performed for $Z \rightarrow \ell^+\ell^-$, $H \rightarrow q\bar{q}'q\bar{q}'$ and $Z \rightarrow q\bar{q}$, $H \rightarrow q\bar{q}'l\nu$ final states achieving a precision of 5 to 2% for Higgs masses between 120 and 160 GeV¹³.

The loop-mediated coupling to photons can be measured best at the photon collider in the reaction $\gamma\gamma \rightarrow H$ with an accuracy of 2% for 120 GeV SM like Higgs boson with 150 fb $^{-1}$ ¹⁴. An alternative method is given by the measurement of $BR(H \rightarrow \gamma\gamma)$. Due to its small value in the SM of 2×10^{-3} the precision for $M_H = 120$ GeV is 23%(16%) for 500 (1000) fb $^{-1}$ exploiting the $\nu\bar{\nu}\gamma\gamma$ and $q\bar{q}\gamma\gamma$ final states¹⁵ at $\sqrt{s} = 500$ GeV.

2.4 Couplings to Fermions and Gluons

The accurate determination of the Higgs couplings to fermions is important as a proof of the Higgs mechanism to be responsible for generating the fermion masses. The partial decay widths

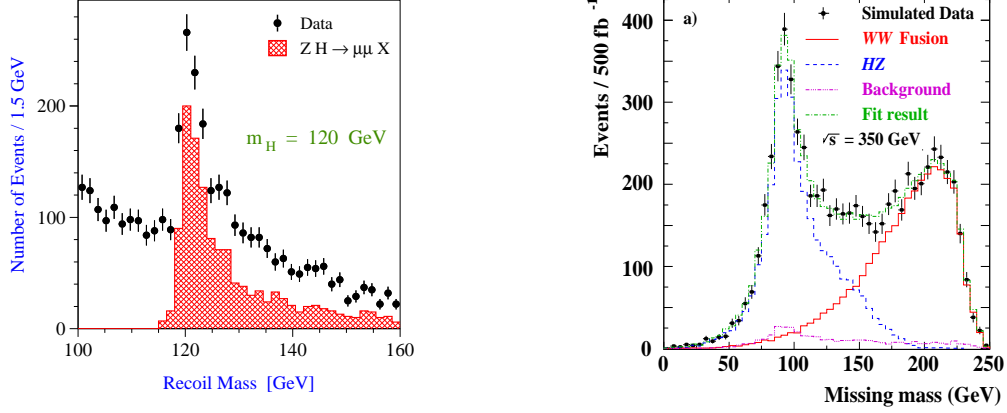


Figure 3: Left: The $\mu^+\mu^-$ recoil mass distribution in the process $e^+e^- \rightarrow ZH \rightarrow X\mu^+\mu^-$ for $M_H = 120$ GeV and 500 fb^{-1} at $\sqrt{s} = 350$ GeV. Right: Simulation of the missing mass distribution in $b\bar{b}\nu\bar{\nu}$ events for 500 fb^{-1} at $\sqrt{s} = 350$ GeV.

to fermions are proportional to $g_{Hf\bar{f}}^2 = m_f^2/v^2$ and are fully determined by the fermions mass in the SM. An observation of deviations from the SM expectations probes the parameters of an extended Higgs sector. The accuracy of the branching ratio measurements relies on the excellent performance of the envisaged vertex detector. In the hadronic Higgs decay channels the fractions of $b\bar{b}$, $c\bar{c}$ and gg final states are extracted by a binned maximum likelihood fit to the jet flavour tagging probabilities for the Higgs boson decay candidates, while the $\tau^+\tau^-$ final states are selected by a dedicated likelihood, based mainly on vertexing and calorimetric response. These measurements are sensitive to the product $\sigma_{ZH,\nu\bar{\nu}H} \times BR(H \rightarrow f\bar{f})$. Using the results discussed above for the production cross-sections the branching ratios can be determined to the following relative accuracies for $M_H = 120$ (140) GeV for 500 fb^{-1} : $b\bar{b}$ 2.4 (2.6)%, $c\bar{c}$ 8.3 (19.0)%, gg 5.5 (14.0)%, $\tau^+\tau^-$ 5.0 (8.0)%¹⁶ (see also Fig. 4 (left)).

The Higgs coupling to the top quark is the largest coupling in the SM ($g_{Ht\bar{t}}^2 \simeq 0.5$ to be compared with $g_{Hb\bar{b}}^2 \simeq 4 \times 10^{-4}$). However, for a light Higgs boson this coupling is accessible indirectly in the loop process $H \rightarrow gg$ and directly only in the Yukawa process $e^+e^- \rightarrow t\bar{t}H$ ¹⁷. This process has a cross-section of the order of only 2.5 fb at $\sqrt{s} = 800$ GeV, including QCD corrections¹⁸. For an integrated luminosity of 1000 fb^{-1} the uncertainty in the Higgs top Yukawa coupling is 5.5%¹⁹. For $M_H \geq 2 \times m_t$ the Higgs top Yukawa couplings can be measured from the $H \rightarrow t\bar{t}$ branching fractions. A study has been performed based on the analysis of the process $e^+e^- \rightarrow \nu_e\bar{\nu}_eH \rightarrow \nu_e\bar{\nu}_et\bar{t}$ for $350 \text{ GeV} < M_H < 500$ GeV at $\sqrt{s} = 800$ GeV yielding an accuracy of 5% (12%) for $M_H = 400$ (500) GeV for an integrated luminosity of 500 fb^{-1} ²⁰.

2.5 Extraction of Higgs Couplings

The Higgs boson production and decay rates discussed above, can be used to measure the Higgs couplings to gauge bosons and fermions. After the Higgs boson is discovered, this is the first crucial step in establishing experimentally the Higgs mechanism for mass generation. Since some of the couplings of interest can be determined independently by different observables while other determinations are partially correlated, it is interesting to perform a global fit to the measurable observables and to extract the Higgs couplings in a model-independent way. This method optimises the available information and can take properly into account the experimental correlation between different measurements. The relative uncertainties on the Higgs boson couplings from this global fit as calculated by HFITTER²¹ are given for $M_H = 120$ GeV and 140 GeV and 500 fb^{-1} in Table 2.5 (see also Fig. 4 (right)).

Table 1: Relative accuracy on Higgs boson couplings obtained from a global fit.

Coupling	g_{HWW}	g_{HZZ}	$g_{Ht\bar{t}}$	$g_{Hb\bar{b}}$	$g_{Hc\bar{c}}$	$g_{H\tau\tau}$
$M_H = 120$ GeV	0.012	0.012	0.030	0.022	0.037	0.033
$M_H = 140$ GeV	0.020	0.013	0.061	0.022	0.102	0.048

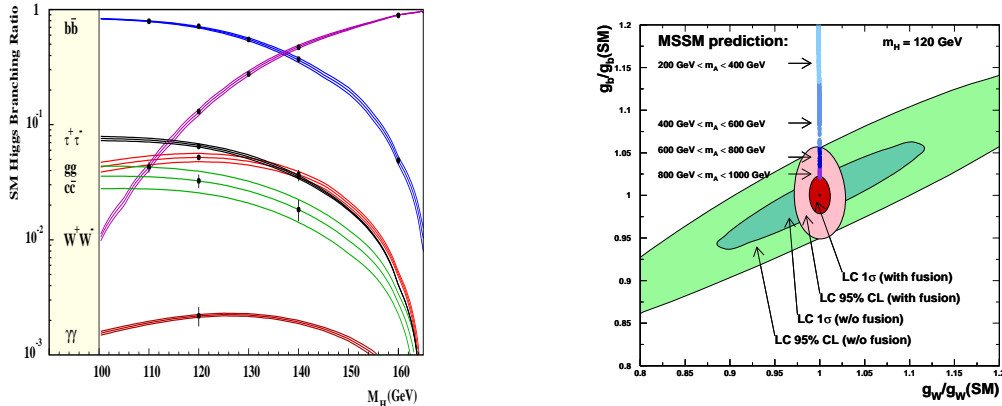


Figure 4: Left: The predicted SM Higgs boson branching ratios. Point with error bars show the expected experimental accuracy, while the lines shows the estimated uncertainties on the SM predictions. Right: Higgs coupling determination from a global fit compared to deviations expected in the MSSM.

2.6 The Total Higgs Width

The total decay width of the Higgs boson is predicted to be too narrow to be resolved experimentally for Higgs boson masses below the ZZ -threshold. Above approximately 200 GeV the total width can be measured directly. For lower masses, indirect methods, exploiting relations between the total decay width and the partial widths for exclusive final states, can be applied: $\Gamma_{\text{tot}} = \Gamma_X/\text{BR}(H \rightarrow X)$. Two feasible options exist for light Higgs bosons: i) the extraction of Γ_{WW} from the measurement of the WW -fusion cross-section combined with the measurement of $\text{BR}(H \rightarrow WW^*)$ and ii) the measurement of the $\gamma\gamma \rightarrow H$ cross-section at a $\gamma\gamma$ collider combined with the measurement of $\text{BR}(H \rightarrow \gamma\gamma)$ in e^+e^- collisions. The WW -fusion option yields a precision on Γ_{tot} of 6% to 13% for Higgs boson masses between 120 and 160 GeV, while the $\gamma\gamma$ option yields a larger error (23% for $M_H = 120$ GeV) dominated by the large uncertainty in the $\text{BR}(H \rightarrow \gamma\gamma)$ determination discussed above. Assuming the $SU(2) \times U(1)$ relation $g_{HWW}^2/g_{HZZ}^2 = 1/\cos^2\theta_W$ to be valid, the measurement of the Higgs-strahlung cross-section provides a viable alternative with potentially higher mass reach than the WW -fusion option. The errors on Γ_{tot} can then be reduced to below 4% for M_H between 140 and 160 GeV.

2.7 The Higgs Potential

In order to fully establish the Higgs mechanism, the Higgs potential $V = \lambda (|\phi|^2 - \frac{1}{2}v^2)^2$ with $v = (\sqrt{2}G_F)^{-1/2} \simeq 246$ GeV must be reconstructed through the determination of the triple, λ_{HHH} , and quartic, λ_{HHHH} , Higgs self couplings. While effects from the quartic coupling may be too small to be observed at the LC, the triple Higgs coupling can be measured in the double Higgs boson production processes $e^+e^- \rightarrow HHZ$ and $\nu_e\bar{\nu}_e HH$. In e^+e^- collisions up to 1 TeV the double Higgs boson associated production with the Z is favoured²². The sensitivity to λ_{HHH} from the measurement of σ_{HHZ} and $\sigma_{\nu\bar{\nu}HH}$ is diluted by the effects of other diagrams, not involving the triple Higgs coupling but leading to the same final state. The huge backgrounds and the small signal cross-section ($\sigma = 0.18$ fb for $M_H = 120$ GeV and $\sqrt{s} = 500$ GeV) make this measurement an experimental challenge. A determination of λ_{HHH} with a statistical accuracy

of 22% for $M_H = 120$ GeV is possible with 1000 fb^{-1} ²³. In the SM the value of λ_{HHH} is fixed after the measurement of the Higgs mass. However, in models with an extra Higgs doublet, additional trilinear Higgs couplings are also present such as λ_{hhH} , λ_{hhA} , λ_{hhh} and λ_{HAA} , which depend also on $\tan\beta$ and M_A and will change the shape of the potential²⁴.

3 SUSY Higgs Bosons

Several extension of the SM model introduce additional Higgs doublets and singlets. A no loose theorem²⁵ guarantees that in a general SUSY model embedded in a GUT scenario at least one Higgs boson will be observable at $\sqrt{s} = 500$ GeV with $\mathcal{L} = 500 \text{ fb}^{-1}$. A specific scenario studied in some detail is the MSSM. The mass reach for pair production of HA and H^+H^- extends to $\approx \sqrt{s}/2 - \epsilon$. This mass range is extended for single production of H and A at a photon collider up to $0.8 \times \sqrt{s_{ee}}$. Establishing the existence of these additional Higgs bosons and the determination of their masses and main decay modes represents an important part of the LC physics program.

3.1 Direct Determination of SUSY Higgs Boson Properties

The decay channels $H, A \rightarrow b\bar{b}, H^+ \rightarrow t\bar{b}$ or $W^+h, h \rightarrow b\bar{b}$ will provide with very distinctive 4 jet and 8 jet final states with 4 b-quark jets that can be efficiently identified and reconstructed. Exemplificative analyses have been performed for these channels, showing that an accuracy of about 0.3% on their mass and of $\simeq 10\%$ on $\sigma \times BR$ can be obtained²⁶. In SUSY models additional decay channels may open. Particularly interesting is the decay of neutral Higgs bosons into an invisible final state *e.g.* $h \rightarrow \chi^0\chi^0$. The comparison of the number of events observed in the $e^+e^- \rightarrow ZH \rightarrow \ell^+\ell^-X$ final state with the sum over the branching ratios of the visible decay modes allows an indirect determination of $BR(H \rightarrow inv.)$ with an accuracy of better than 20% for $BR(H \rightarrow inv.) \geq 0.05$.

3.2 Indirect Determination of SM/MSSM Nature of a Light Higgs Boson

The discovery of a neutral Higgs boson, with mass in the range $115 \text{ GeV} < M_H < 140 \text{ GeV}$, will raise the question of whether the observed particle is the SM Higgs boson or the lightest boson from the Higgs sector of a SM extension. It has been shown that, for a large fraction of the $\tan\beta - M_A$ parameter plane in the MSSM, this neutral boson will be the only Higgs state observed at the LHC (see Fig. 5 (left)). In this circumstance, a Higgs particle generated by a complex multi-doublet model could be indirectly recognised only by a study of its couplings. If the HZZ coupling, measured by the Higgs-strahlung production cross-section independently from the Higgs boson decay mode, turns out to be significantly smaller than the SM expectation, this will signal the existence of extra Higgs doublets.

The determination of the Higgs boson decay branching ratios with the accuracy anticipated by these studies can be employed to identify the SM or MSSM nature of a light neutral Higgs boson, because the Higgs boson decay widths to a specific final state are modified by factors involving $\tan\beta$ and α in the MSSM compared to the SM. Therefore, deviations in the ratios of branching ratios such as *e.g.* $\frac{BR(h \rightarrow WW^*)}{BR(h \rightarrow b\bar{b})}$ from their SM expectations can reveal the MSSM nature of the Higgs boson and also provide indirect information on the mass of the CP -odd A^0 Higgs boson, even when it is so heavy that it can not be directly observed at $\sqrt{s} = 500$ GeV.

To compare the SM predictions with those in MSSM, a complete scan of the MSSM parameter space has been performed for $M_h = (120 \pm 2)$ GeV. It was found that for $M_A \leq 600$ GeV 95% of the MSSM solutions can be excluded at 95% confidence level^{16,27}. In the case of an significant deviation from the SM expectation this can be translated into an indirect determination of M_A yielding an accuracy of 70 to 100 GeV for $300 \text{ GeV} < M_A < 600 \text{ GeV}$.

4 The Complementarity with the LHC

At the LHC the SM Higgs boson, or at least one Higgs boson in the MSSM, will be observed. Beyond its discovery a limited number of measurements of Higgs boson properties can be carried out at the LHC (mass, total width for a heavy Higgs boson, some ratios of couplings). Further perspectives for the observation of an invisible decaying Higgs, and measurements of the total width for lower masses and of the g_{HWW} coupling have been recently suggested for the LHC²⁸.

The complementarity of the linear collider data to the picture of the Higgs sector as it will have been outlined by the LHC is therefore threefold. First the accuracy of those measurements, which are possible at the LHC, can be significantly increased for e.g. $M_H = 120$ (160) GeV: $\Delta M/M = 9$ (10) $\times 10^{-4}$ at the LHC and 3 (4) $\times 10^{-4}$ at the LC, $g_{Ht\bar{t}}/g_{HWW} = 0.070$ at the LHC and 0.023 at the LC, $g_{Hb\bar{b}}/g_{HWW} = 0.050$ at the LHC and 0.022 at the LC. Secondly the absolute measurements of all the relevant Higgs boson couplings, including the Higgs self coupling, will be possible only at the LC. Finally extended Higgs sector scenarios (e.g. invisible Higgs boson decays or 2HDM) can be observed at the linear collider closing the loopholes of a possible non-discovery at the LHC.

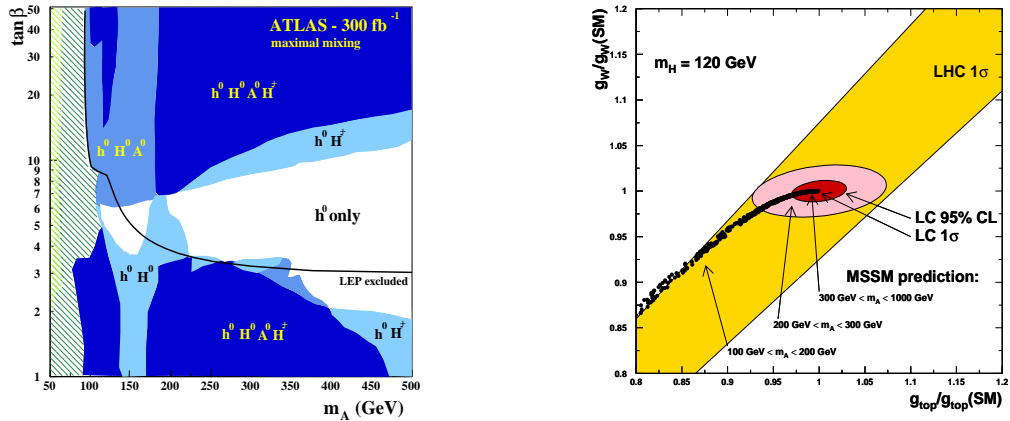


Figure 5: Left: Higgs bosons which are observable in ATLAS with 300 fb^{-1} in the maximal mixing scenario of the MSSM. In the white region only the lightest boson is observable if only SM-like decays are accessible. At the LC the SM or MSSM nature of the h boson can be distinguished from the precision measurements for the entire area. Right: A comparison of the accuracy in the determination of the $g_{ht\bar{t}}$ and g_{HWW} Higgs couplings at the LHC and the LC compared to the predictions from the MSSM.

5 Summary

The search for the Higgs boson and the study of its properties is one of the main goals of present research in particle physics. The central role of a linear collider in the understanding of the mechanism of electroweak symmetry breaking, complementing the data to be acquired at the Tevatron and at the LHC, has been clearly outlined by the studies carried out world-wide.

Acknowledgements

I am grateful to the organisers especially to J. Tran Thanh Van for their invitation and the inspiring atmosphere. The results reported here are due to the activities of many colleagues, in the regional Higgs working groups of the Worldwide Study on Physics at Linear Colliders, whose contributions are gratefully acknowledged.

References

1. P.W.Higgs, *Phys. Rev. Lett.* **12** (1964) 132; *idem*, *Phys. Rev.* **145** (1966) 1156; F.Englert and R.Brout, *Phys. Rev. Lett.* **13** (1964) 321; G.S.Guralnik, C.R.Hagen and T.W.Kibble, *Phys. Rev. Lett.* **13** (1964) 585.
2. ALEPH, DELPHI, L3 and OPAL Collaborations, LEP Higgs Working Group, *Search for the Standard Model Higgs Boson at LEP*, CERN-EP/2001-055, July 2001.
3. M.Carena *et al.*, *Report of the Tevatron Higgs working group*, hep-ph/0010338.
4. D.Costanzo, these proceedings.
5. *TESLA Technical Design Report Part 3: Physics at an e^+e^- Linear Collider*, R.D.Heuer *et al.* (ed.), DESY-2001-011, hep-ph/0106315.
6. *Linear Collider Physics Resource Book for Snowmass 2001 PART 2: Higgs and Supersymmetry Studies*, T.Abe *et al.* (ed.), BNL-52627, hep-ex/0106056.
7. P.Garcia-Abia, W.Lohmann, A.Raspereza. LC-PHSM-2001-054; J.-C.Brient. LC-PHSM-2000-049.
8. D.J.Miller *et al.*, LC-TH-2001-033.
9. M.T.Dova, P.Garcia-Abia, W.Lohmann. LC-PHSM-2001-054.
10. A.Djouadi and B.A.Kniehl, DESY 93-123C, 51.
11. M.Schumacher, LC-PHSM-2001-003.
12. K.Desch and N.Meyer, LC-PHSM-201-025.
13. G.Borisov and F.Richard, Note LAL 99-26 and hep-ph/9905413.
14. G.Jikia and S.Söldner-Rembold, *Nucl. Phys. Proc. Suppl.* **82** (2000) 373, LC-PHSM-2001-060.
15. E.Boos *et al.*, DESY-00-162, LC-PHSM-2000-053.
16. M.Battaglia, in Proc. of the *Worldwide Study on Physics and Experiments with Future e^+e^- Linear Colliders*, E.Fernandez and A.Pacheco (editors), UAB, Barcelona 2000, vol. I, 163 and hep-ph/9910271.
17. A.Djouadi, J.Kalinowski and P.M.Zerwas, *Mod. Phys. Lett.* **A7** (1992) 1765 and *Z. Phys.* **C54** (1992) 255.
18. S.Dittmaier *et al.*, *Phys. Lett.* **B 478**, (2000), 247; S.Dawson, L.Reina, *Phys. Rev.* **D 59**, (1999), 054012.
19. A.Juste and G.Merino, *Top-Higgs Yukawa Coupling measurement at a Linear e^+e^- Collider*, hep-ph/9910301; H.Baer, S.Dawson, L.Reina *Phys. Rev.* **D61**, (2000), 013002.
20. J.Alcaarez and E.Ruiz Morales, *Measuring the Top Yukawa Coupling to a heavy Higgs Boson at a future e^+e^- Linear Collider*, hep-ph/0012109.
21. K.Desch and M.Battaglia, LC-PHSM-2001-053.
22. A.Djouadi *et al.*, *Eur. Phys. J.* **C10** (1999) 27.
23. C.Castanier *et al.*, LC-PHSM-2000-061.
24. G.Gounaris, A.Djouadi, H.E.Haber and P.M.Zerwas, *Phys. Lett.* **B375** (1996) 203; A.Djouadi *et al.*, *Eur. Phys. J.* **C10** (1999) 27.
25. J.R.Espinosa, J.F.Gunion. *Phys. Rev. Lett.* **82** (1999) 1084.
26. A.Kiiskinen, M.Battaglia and P.Pöyhönen, LC-PHSM-2001-041; A.Andreaazza and C.Trincon, DESY-123-E, 417.
27. a similar study can be found in: M.Carena *et al.*, *Distinguishing a MSSM Higgs Boson from the SM Higgs Boson at a Linear Collider*, hep-ph/0106116.
28. O.J.P.Eboli, D.Zeppenfeld, *Phys. Lett.* **B495**, (2000), 147; D.Zeppenfeld *et al.*, *Phys. Rev.* **D62** (2000) 13009.